Polarization singularities in near-field of Gaussian vortex beam diffracted by a circular aperture*

Li Jian-Long(李建龙)†

College of Physical Science and Technology, Sichuan University, Chengdu 610064, *China*

(Received 8 April 2010; revised manuscript received 27 May 2010)

Polarization singularities in the near-field of Gaussian vortex beams diffracted by a circular aperture are studied by a rigorous electromagnetic theory. It is shown that there exist C-points and L-lines, which depend on off-axis displacement parameters along the x and y directions, waist width, wavelength, and topological charge of the diffracted Gaussian vortex beam, as well as on propagation distance. The results are illustrated by numerical calculations.

Keywords: polarization singularities, rigorous electromagnetic field theory, Gaussian vortex beams

PACC: 4000, 4225B

1. Introduction

There has been substantial interest in polarization singularities which as typical singularities in vector wave fields have been extensively studied both analytically and experimentally since Nye's work.[1−10] However, to our knowledge, there has been no study on polarization singularities in the near field of the Gaussian vortex beam diffracted by a circular aperture. This may be because the solving of the light field in the near-field or the sub-wavelength region needs to use the rigorous electromagnetic field and consider the actual characteristics of the boundary condition. Based on a rigorous electromagnetic field theory and the Fourier series, the polarization singularities in the near-field of the Gaussian vortex beam diffracted by a circular aperture are studied, and the Stokes parameters are improved in this paper. Numerical calculations show that polarization singularities depend on off-axis displacement parameters along the x and y directions, waist width, wavelength and topological charge of the Gaussian vortex beams, as well as on the propagation distance. Certainly, this theory proposed in this paper can also be employed to study the distribution of phase singularities in the near-field region of the electromagnetic field diffracted by other surface-shaped apertures.

2. Rigorous electromagnetic theory of Gaussian vortex beam diffracted by circular aperture

As shown in Fig. 1, a Gaussian beam carrying an optical vortex is incident onto a diffraction screen of a circular aperture (radius u), and the aperture plane is perpendicular to the z axis. The diffraction process can be divided into three regions, these being incidence region I ($z < 0$), diffraction region II ($z = 0$) and transmission region III ($z > 0$). The electric field of the beam incident onto the plane $z = 0$ can be expressed as

$$\begin{aligned}&\boldsymbol{E}_x(\rho_0,\theta_0,0)\\ &= E_0[(\rho_0\cos\theta_0 - a)\\ &\quad + \mathrm{i}\,\mathrm{sgn}(m)(\rho_0\sin\theta_0 - b)]^{|m|}\exp\left(-\frac{\rho_0^2}{w_0^2}\right), \quad (1a)\\ &\boldsymbol{E}_y(\rho_0,\theta_0,0) = 0, \quad (1b)\end{aligned}$$

where w_0 is the waist width of the Gaussian beam, m is the topological charge ($m = \pm 1$ in this paper), a and b denote the off-axis displacement parameters along the x and the y directions, respectively, E_0 is a constant, and (ρ_0, θ_0) is the cylindrical coordinate in the source plane $z = 0$. From Eq. (1), the parameters of w_0, a, b and m all affect the incident electric field. It is known that the electromagnetic fields in the three regions can be obtained by superpositing

*Project supported by the China Postdoctoral Science Foundation (Grant No. 2009450159), and the Foundation of the State Key Laboratory of Optical Technologies for Micro-Frabrication and Micro-Engineering, Chinese Academy of Sciences (Grant No. KF001).

†Corresponding author. E-mail: sculjl@163.com

© 2010 Chinese Physical Society and IOP Publishing Ltd

the basic modal fields of the TE and TM waves, and the transverse component of the incident electric field (expressed as $\boldsymbol{E}_{\rm t}^{i}(\rho,\theta)$) can be expressed as

$$\boldsymbol{E}_{\rm t}^{\rm in}(\rho,\theta)=\sum_{d=1}^{2}\iint {\rm d}p{\rm d}q\boldsymbol{A}_{d}^{\rm in}(p,q)\boldsymbol{\Phi}_{d1}(p,q), \quad (2)$$

where $\boldsymbol{A}_{1}^{\rm in}(p,q)$ and $\boldsymbol{A}_{2}^{\rm in}(p,q)$ can be obtained from the Fourier transform of Eq. (1), and denote the amplitudes of the incident waves TE and TM, respectively; p and q respectively denote the skewness factors of the incident field along the x axis and the y axis; α and β respectively represent the angle between the z axis and the incident direction and one between the x axis and the incident plane.

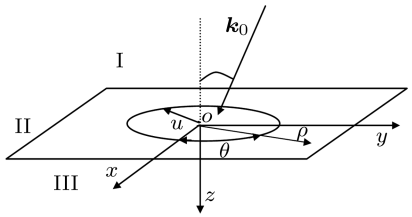


Fig. 1. Schematic illustration of a beam diffracted by a circular aperture.

$$\boldsymbol{\Phi}_{11}(p,q)=\hat{P}_x\exp[{\rm i}k_0(p\rho\cos\theta+q\rho\sin\theta+m(p,q)z)], \quad (3a)$$

$$\boldsymbol{\Phi}_{12}(p,q)=\hat{P}_x\exp[{\rm i}k_0(p\rho\cos\theta+q\rho\sin\theta-m(p,q)z)], \quad (3b)$$

$$\boldsymbol{\Phi}_{21}(p,q)=\hat{P}_y\exp[{\rm i}k_0(p\rho\cos\theta+q\rho\sin\theta+m(p,q)z)], \quad (3c)$$

$$\boldsymbol{\Phi}_{22}(p,q)=\hat{P}_y\exp[{\rm i}k_0(p\rho\cos\theta+q\rho\sin\theta-m(p,q)z)], \quad (3d)$$

where $\boldsymbol{P}_x$ and $\boldsymbol{P}_y$ denote the unit vectors of transverse components of the electromagnetic field, and can be expressed as follows:

$$\boldsymbol{P}_x=\frac{(q\cos\theta-p\sin\theta)\boldsymbol{\rho}-(q\sin\theta+p\cos\theta)\boldsymbol{\theta}}{p^2+q^2}, \quad (4a)$$

$$\boldsymbol{P}_y=\frac{(p\cos\theta+q\sin\theta)\boldsymbol{\rho}-(p\sin\theta-q\cos\theta)\boldsymbol{\theta}}{p^2+q^2}. \quad (4b)$$

The transverse component of the electric field (expressed as $\boldsymbol{E}_{\rm t}^{\rm I}(\rho,\theta)$) in region I can be expressed as

$$\boldsymbol{E}_{\rm t}^{\rm I}(\rho,\theta)=\boldsymbol{E}_{\rm t}^{\rm in}(\rho,\theta)+\sum_{d=1}^{2}\iint {\rm d}p{\rm d}q\boldsymbol{A}_{d}^{\rm in}(p,q)\boldsymbol{\Phi}_{d2}(p,q). \quad (5)$$

And the electromagnetic field in region III can be given by

$$\boldsymbol{E}_{\rm t}^{\rm III}(\rho,\theta)=\sum_{d=1}^{2}\iint {\rm d}p{\rm d}q\boldsymbol{A}_{d}^{\rm tr}(p,q)\boldsymbol{\Phi}_{d1}(p,q), \quad (6)$$

$$Z_0\boldsymbol{z}\times\boldsymbol{H}_{\rm t}^{\rm III}(\rho,\theta)=\sum_{d=1}^{2}\iint {\rm d}p{\rm d}qY_d(p,q)\boldsymbol{A}_{d}^{\rm tr}(p,q)\boldsymbol{\Phi}_{d1}(p,q), \quad (7)$$

where $\boldsymbol{A}_{1}^{\rm tr}(p,q)$ and $\boldsymbol{A}_{2}^{\rm tr}(p,q)$ denote the amplitudes of the TE and the TM waves in region III, respectively. From Ref. [11], the transverse component of the electromagnetic field in the circular aperture area can be written as follows:

$$\boldsymbol{E}_{\rm t}^{\rm II}(\rho,\theta)=\sum_{s=1}^{2}\sum_{n=0}^{\infty}\sum_{m=1}^{\infty}\sum_{l=1}^{2}[b_{snml}\cos(k_0v_{smn}z)]\boldsymbol{\Psi}_{snml}(\rho,\theta), \quad (8)$$

and the magnetic field can be expressed as

$$Z_0\boldsymbol{z}\times\boldsymbol{H}_{\rm t}^{\rm II}(\rho,\theta)={\rm i}\sum_{snml}[\Lambda_{snm}a_{snml}\cos(k_0v_{snm}z)]\boldsymbol{\Psi}_{snml}(\rho,\theta), \quad (9)$$

where

$$v_{1nm}=\sqrt{1-(\chi_{nm'})^2/(k_0u)^2},$$
$$\Lambda_{1nm}=v_{1nm},\quad \chi_{nm'}=J_{m'}(n), \quad (10a)$$
$$v_{2nm}=\sqrt{1-(\chi_{nm})^2/(k_0u)^2},$$
$$\Lambda_{21nm}=1/v_{2nm},\quad \chi_{nm}=J_{m}(n). \quad (10b)$$

Certainly, the electric fields in these regions are matched in the plane $z=0$ by imposing the continuity of the transverse component of the electromagnetic field in appropriate domains. By using Eqs. (5), (6) and (8), the continuity of transverse electric fields in the interface $z=0$ is specified by

$$\sum_{d=1}^{2}\iint {\rm d}p{\rm d}q[\boldsymbol{\Phi}_{d1}(p,q)+\boldsymbol{\Phi}_{d2}(p,q)]\boldsymbol{A}_{d}^{\rm in}(p,q)_{z=0}=\sum_{snml}b_{snml}\boldsymbol{\Psi}_{snml}(\rho,\theta)\ \ \text{(inside the hole)}, \quad (11a)$$

$$\sum_{d=1}^{2}\iint {\rm d}p{\rm d}q[\boldsymbol{\Phi}_{d1}(p,q)+\boldsymbol{\Phi}_{d2}(p,q)]\boldsymbol{A}_{d}^{\rm in}(p,q)=0\ \ \text{(outside the hole)}. \quad (11b)$$

In the interface $z = 0$, the magnetic field $\boldsymbol{z} \times \boldsymbol{H}_{\mathrm{t}}^{\mathrm{II}}$ satisfies

$$\sum_{d=1} \iint \mathrm{d}p\mathrm{d}q[\boldsymbol{\Phi}_{d1}(p,q) - \boldsymbol{\Phi}_{d2}(p,q)]\boldsymbol{A}_d^{\mathrm{in}}(p,q)_{z=0} = -\mathrm{i}\sum_{snml} \Lambda_{snm} a_{snml} \boldsymbol{\Psi}_{snml}(\rho,\theta)_{z=0} \quad \text{(inside the hole)}. \tag{12}$$

According to Maxwell's equations, the components of the transverse electric field satisfies the following equations:

$$\begin{aligned} &\frac{\partial \boldsymbol{E}_y^{\mathrm{I}}(\rho,\theta)}{\partial\rho}\frac{1}{\cos\theta} - \frac{\partial \boldsymbol{E}_y^{\mathrm{I}}(\rho,\theta)}{\partial\theta}\frac{1}{\rho\sin\theta} - \frac{\partial \boldsymbol{E}_x^{\mathrm{I}}(\rho,\theta)}{\partial\rho}\frac{1}{\sin\theta} - \frac{\partial \boldsymbol{E}_x^{\mathrm{I}}(\rho,\theta)}{\partial\theta}\frac{1}{\rho\cos\theta} \\ &= \frac{\partial \boldsymbol{E}_y^{\mathrm{II}}(\rho,\theta)}{\partial\rho}\frac{1}{\cos\theta} - \frac{\partial \boldsymbol{E}_y^{\mathrm{II}}(\rho,\theta)}{\partial\theta}\frac{1}{\rho\sin\theta} - \frac{\partial \boldsymbol{E}_x^{\mathrm{II}}(\rho,\theta)}{\partial\rho}\frac{1}{\sin\theta} - \frac{\partial \boldsymbol{E}_x^{\mathrm{II}}(\rho,\theta)}{\partial\theta}\frac{1}{\rho\cos\theta}, \end{aligned} \tag{13a}$$

$$\begin{aligned} &\frac{\partial \boldsymbol{E}_y^{\mathrm{II}}(\rho,\theta)}{\partial\rho}\frac{1}{\cos\theta} - \frac{\partial \boldsymbol{E}_y^{\mathrm{II}}(\rho,\theta)}{\partial\theta}\frac{1}{\rho\sin\theta} - \frac{\partial \boldsymbol{E}_x^{\mathrm{II}}(\rho,\theta)}{\partial\rho}\frac{1}{\sin\theta} - \frac{\partial \boldsymbol{E}_x^{\mathrm{II}}(\rho,\theta)}{\partial\theta}\frac{1}{\rho\cos\theta} \\ &= \frac{\partial \boldsymbol{E}_y^{\mathrm{III}}(\rho,\theta)}{\partial\rho}\frac{1}{\cos\theta} - \frac{\partial \boldsymbol{E}_y^{\mathrm{III}}(\rho,\theta)}{\partial\theta}\frac{1}{\rho\sin\theta} - \frac{\partial \boldsymbol{E}_x^{\mathrm{III}}(\rho,\theta)}{\partial\rho}\frac{1}{\sin\theta} - \frac{\partial \boldsymbol{E}_x^{\mathrm{III}}(\rho,\theta)}{\partial\theta}\frac{1}{\rho\cos\theta}. \end{aligned} \tag{13b}$$

By employing the Parseval theorem,[12] equations (13a) and (13b) can be transformed as follows:

$$\begin{aligned} &\frac{\partial \hat{E}_y^{\mathrm{I}}(\rho,\theta)}{\partial\rho}\frac{1}{\cos\theta} - \frac{\partial \hat{E}_y^{\mathrm{I}}(\rho,\theta)}{\partial\theta}\frac{1}{\rho\sin\theta} - \frac{\partial \hat{E}_x^{\mathrm{I}}(\rho,\theta)}{\partial\rho}\frac{1}{\sin\theta} - \frac{\partial \hat{E}_x^{\mathrm{I}}(\rho,\theta)}{\partial\theta}\frac{1}{\rho\cos\theta} \\ &= \frac{\partial \hat{E}_y^{\mathrm{II}}(\rho,\theta)}{\partial\rho}\frac{1}{\cos\theta} - \frac{\partial \hat{E}_y^{\mathrm{II}}(\rho,\theta)}{\partial\theta}\frac{1}{\rho\sin\theta} - \frac{\partial \hat{E}_x^{\mathrm{II}}(\rho,\theta)}{\partial\rho}\frac{1}{\sin\theta} - \frac{\partial \hat{E}_x^{\mathrm{II}}(\rho,\theta)}{\partial\theta}\frac{1}{\rho\cos\theta}, \end{aligned} \tag{14a}$$

$$\begin{aligned} &\frac{\partial \hat{E}_y^{\mathrm{II}}(\rho,\theta)}{\partial\rho}\frac{1}{\cos\theta} - \frac{\partial \hat{E}_y^{\mathrm{II}}(\rho,\theta)}{\partial\theta}\frac{1}{\rho\sin\theta} - \frac{\partial \hat{E}_x^{\mathrm{II}}(\rho,\theta)}{\partial\rho}\frac{1}{\sin\theta} - \frac{\partial \hat{E}_x^{\mathrm{II}}(\rho,\theta)}{\partial\theta}\frac{1}{\rho\cos\theta} \\ &= \frac{\partial \hat{E}_y^{\mathrm{III}}(\rho,\theta)}{\partial\rho}\frac{1}{\cos\theta} - \frac{\partial \hat{E}_y^{\mathrm{III}}(\rho,\theta)}{\partial\theta}\frac{1}{\rho\sin\theta} - \frac{\partial \hat{E}_x^{\mathrm{III}}(\rho,\theta)}{\partial\rho}\frac{1}{\sin\theta} - \frac{\partial \hat{E}_x^{\mathrm{III}}(\rho,\theta)}{\partial\theta}\frac{1}{\rho\cos\theta}, \end{aligned} \tag{14b}$$

where $\hat{E}^{\mathrm{I}}$ and $\hat{E}^{\mathrm{II}}$ denote the Fourier transforms of $\boldsymbol{E}^{\mathrm{I}}$ and $\boldsymbol{E}^{\mathrm{II}}$, respectively. When n and m in Eqs. (11) and (13) approach infinity, the electric field obtained is exact. For the incident wavelength comparable to the circular radius u in this paper, the electric field distributions expressed by Eqs. (11) and (13) are invariant when m and n reach some small values. With some finite truncation term numbers of m and n, a_{snml} and b_{snml} can be solved according to Eqs. (13) and (14). Then transverse components of electromagnetic magnetic fields in region III expressed as Eqs. (11) and (13) can be obtained. Based on Maxwell's equations, the z component of the electromagnetic field in region III can be obtained as follows:

$$\boldsymbol{E}_z(\rho,\theta) = \int_0^{+R} \left[\frac{\partial E_x^{\mathrm{III}}(\rho,\theta)}{\partial\rho}\frac{1}{\cos\theta} - \frac{\partial E_x^{\mathrm{III}}(\rho,\theta)}{\partial\theta}\frac{1}{\rho\sin\theta} + \frac{\partial E_y^{\mathrm{III}}(\rho,\theta)}{\partial\rho}\frac{1}{\sin\theta} + \frac{\partial E_y^{\mathrm{III}}(\rho,\theta)}{\partial\theta}\frac{1}{\rho\cos\theta}\right]\mathrm{d}z, \tag{15a}$$

$$\boldsymbol{H}_z(\rho,\theta) = \int_0^{+R} \left[\frac{\partial H_x^{\mathrm{III}}(\rho,\theta)}{\partial\rho}\frac{1}{\cos\theta} - \frac{\partial H_x^{\mathrm{III}}(\rho,\theta)}{\partial\theta}\frac{1}{\rho\sin\theta} + \frac{\partial H_y^{\mathrm{III}}(\rho,\theta)}{\partial\rho}\frac{1}{\sin\theta} + \frac{\partial H_x^{\mathrm{III}}(\rho,\theta)}{\partial\theta}\frac{1}{\rho\cos\theta}\right]\mathrm{d}z, \tag{15b}$$

where R denotes the distance between the viewing-screen and the diffraction screen, and the diffraction electric field of the circular aperture can be determined according to Eqs. (11)–(13) and (15).

When the Gaussian vortex beam is incident onto the circular aperture located in the x–z plane, the diffractive electric field can be rewritten as

$$\boldsymbol{E}(\rho,z) = E_s(\rho,z)\boldsymbol{s} + E_z(\rho,z)\boldsymbol{k}, \tag{16}$$

where $\boldsymbol{s}$ denotes the unit resultant direction of the unit direction along the x axis and the y axis, and

$$\boldsymbol{E}_s(\rho,z) = [\boldsymbol{E}_x^2(\rho,z) + \boldsymbol{E}_y^2(\rho,z)]^{1/2} \tag{16a}$$

denotes the resultant amplitude of $E_x(\rho,z)$ and $E_y(\rho,z)$, and $\boldsymbol{k}$ denotes the unit vector along the z axis. Then some parameters of the diffraction field can be written in the forms as given from their conventional definitions, i.e.,

$$\alpha_1 = |E_z(\rho,z)|, \tag{17}$$

$$\delta_1 = \arg[E_z(\rho, z)], \tag{18}$$

$$\alpha_2 = |E_s(\rho, z)|, \tag{19}$$

$$\delta_2 = \arg[E_s(\rho, z)], \tag{20}$$

where α_1 and α_2 respectively denote the transverse and the longitudinal intensities of the electromagnetic field. δ_2 and δ_1 respectively represent the azimuthal angles of the horizontal and the vertical components of the electromagnetic field. Thus, the Stokes parameters are defined as

$$S_0 = \alpha_1^2 + \alpha_2^2, \tag{21}$$

$$S_1 = \alpha_1^2 - \alpha_2^2, \tag{22}$$

$$S_2 = 2\alpha_1\alpha_2 \cos\delta, \tag{23}$$

$$S_3 = 2\alpha_1\alpha_2 \sin\delta. \tag{24}$$

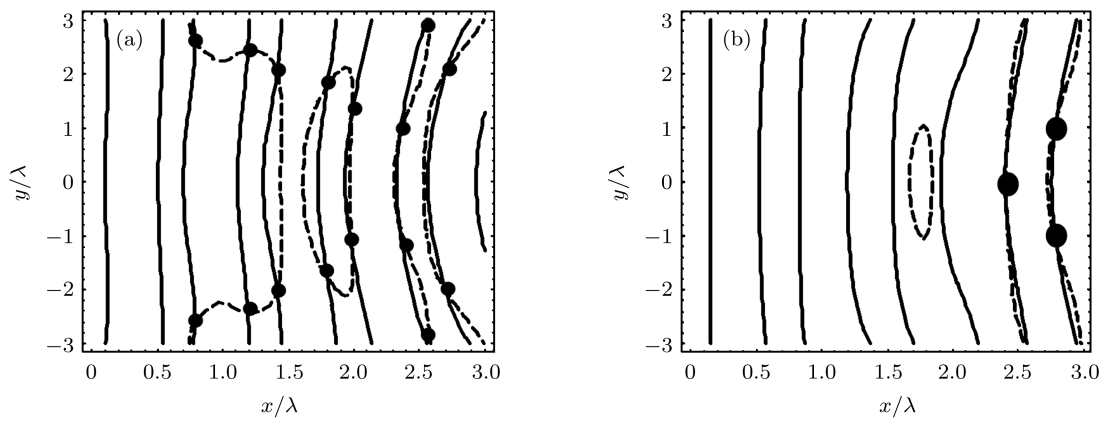
It is easy to see that the Stokes parameters expressed by Eqs. (21)–(24) are related to the amplitudes of the components of the electric field $\boldsymbol{E}_z$ and $\boldsymbol{E}_s$, and resolved in two perpendicular directions normal to the direction of propagation. In Eqs. (23) and (24), $\delta = \delta_2 - \delta_1$. The parameter S_0 is a measure of the total power in the wave, S_1 and S_2 represent the linearly polarized components, and S_3 denotes the circularly polarized component. These values can be converted into a measure of the polarization. In a way similar to that in Ref. [13], equations (21)–(24) can be used to describe the polarization singularities of the diffraction field. At C-points the polarization ellipse reduces into a circle, thus the orientations of the major and the minor axes of the polarization ellipse are undetermined. Therefore, $s_1 = s_2 = 0$ (i.e., the complex Stokes field $s_{12} = s_1 + \mathrm{i}s_2 = 0$) corresponds to C-points, and $s_3 = \pm 1$ refer to right-($s_3 = +1$) handiness and left-($s_3 = -1$) handiness, respectively. If the polarization ellipse degenerates into a line, the right-(left-) handiness of the polarization ellipse degenerates into a line, thus the right- (left-) handiness of the polarization ellipse is undetermined. From Eq. (24) it follows that $s_3 = 0$, i.e.,

$$\begin{aligned}&\mathrm{Re}[E_z(x, y, z)]\mathrm{Im}[E_s(x, y, z)]\\ &- \mathrm{Re}[E_s(x, y, z)]\mathrm{Im}[E_z(x, y, z)] = 0.\end{aligned} \tag{25}$$

3. Numerical calculation and analysis

Consider the optical parameters of $\lambda = 1.06$ μm, $w_0 = 1.0$ mm, $a = -0.5w_0$ and $b = 0.2w_0$ to be fixed. The distributions of the C-points and L-lines are shown in the following figures.

Figure 2 shows the distributions of C-points of the diffraction field at different propagation distances when the radius of the circular aperture $u = 10\lambda$. As indicated in Fig. 2(a), there exist 16 C-points in the observation zone $x \in (0, 3\lambda)$ and $y \in (-3\lambda, 3\lambda)$ in the plane $z = 3\lambda$, and these C-points have a symmetric distribution along the x axis. Comparing panels in Fig. 2, we find that the propagation distance has a greater influence on the distribution of C-points in the diffraction field, and the number of C-points in the observation region decreases from 16 to 0 with the diffractive propagation distance increasing. But there are no C-points in the observation region when the observation distance is more than 10λ. This result may be explained by employing the broadening effect of the aperture diffraction of the light field, and thus it leads these C-points to move away from the observation region.



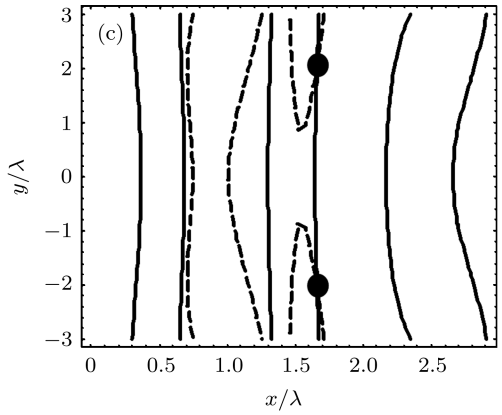


Fig. 2. Distributions of C-points in the diffraction field in different planes with the radius of the circular aperture $u = 10\lambda$: (a) $z = 3\lambda$, (b) $z = 5\lambda$, and (c) $z = 8\lambda$.

Figure 3 shows the distribution of C-points of the diffraction field in the plane $z = 3\lambda$ with the radius of the circular aperture $u = 4\lambda$. As shown in Fig. 3, there exist 14 C-points in the observation region $x \in (0, 3\lambda)$ and $y \in (-3\lambda, 3\lambda)$. By comparison with Fig. 2(a), it is shown that the radius of the circular aperture has an effect on the distribution of the C-points, and its distribution in Fig. 3 is different from that in Fig. 2(a).

Figure 4 displays the distributions of L-lines in the diffraction field in different planes. As shown in Fig. 4(a), there exist many L-lines in the observation region in the plane $z = 3\lambda$. But the number of the L-lines decreases with the increase of distance from observation plane ($z = 8\lambda$) for the diffraction broadening effect of the aperture diffraction.

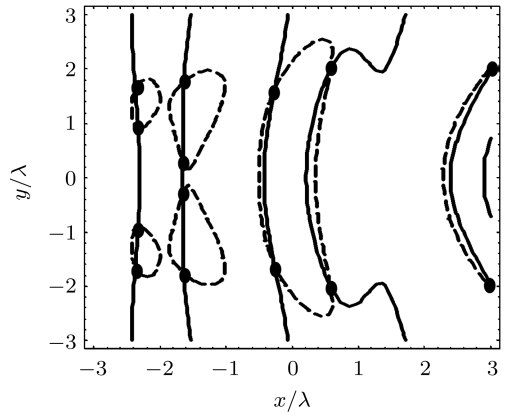


Fig. 3. Distribution of C-points in the diffraction field in the plane $z = 3\lambda$ with the radius of the circular aperture $u = 4\lambda$.

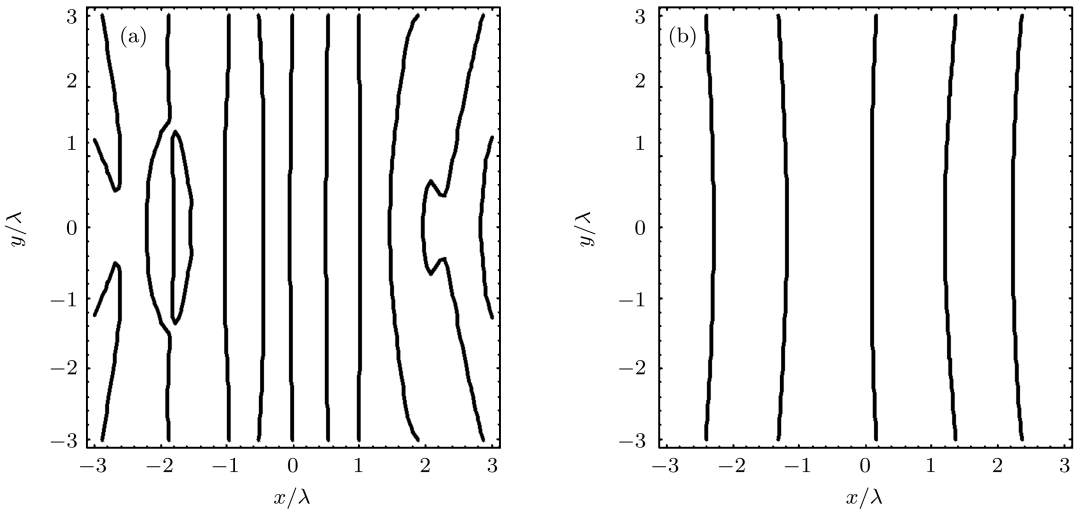


Fig. 4. Distributions of L-lines in the diffraction field in two planes with the radius $u = 4\lambda$:. (a) $z = 3\lambda$, and (b) $z = 8\lambda$.

Figure 5 exhibits the distribution of $L-$lines in the diffraction field in the plane $z = 8\lambda$ with the radius of the aperture $u = 10\lambda$. Figure 5 shows that the number of the L-lines is more than that in Fig. 4(b). This may be because the radius of the circular aperture in Fig. 5 is more than that in Fig. 4(b), and the diffraction broadening effect is much less than that in Fig. 4(b).

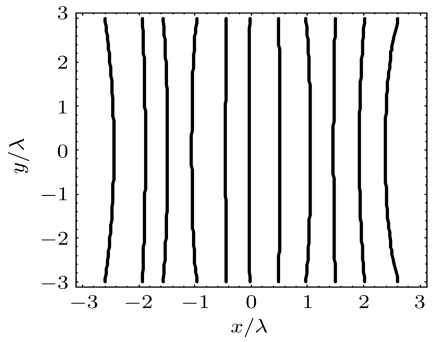


Fig. 5. Distribution of L-lines in the diffraction field in the plane $z = 8\lambda$ with the radius $u = 10\lambda$.

4. Conclusion

Based on the rigorous electromagnetic field theory, polarization singularities in the near field of the diffraction field of the Gaussian vortex beam diffracted by the circular aperture are studied in this paper. The numerical calculations show that there exist C-points and L-lines, which depend on off-axis displacement parameters along the x and the y directions, waist width, wavelength, radius of the aperture, as well as on the propagation distance in the diffraction near-field. It is noticeable to point out that in order to explain the main physical problem, polarization singularities in the nea-field of the Gaussian vortex beam diffraction by a circular aperture are taken as example. The rigorous theory in this paper can be used to study polarization singularities in the near-field of the other beams diffracted by other shaped apertures.

References

[1] Nye J F 1999 *Natural Focusing and the Fine Structure of Light* (Bristol: IOP Publishing)

[2] Berry M V and Dennis M R 2001 *Proc. R. Soc. London Ser.* A **457** 141

[3] Wheeldon J F and Schriemer H 2009 *Opt. Express* **17** 2111

[4] Bliokh K Y, Niv A, Kleiner V and Hasman E 2008 *Opt. Express* **16** 695

[5] Dennis M R 2008 *Opt. Lett.* **33** 2572

[6] Schoonover R W and Visser T D 2006 *Opt. Express* **14** 5733

[7] Flossmann F, Schwarz U T, Maier M and Dennis M R 2005 *Phys. Rev. Lett.* **95** 253901

[8] Soskin M S, Denisenko V and Freund I 2003 *Opt. Lett.* **28** 1475

[9] Mokhun A I, Soskin M S and Freund I 2002 *Opt. Lett.* **27** 995

[10] Li J L 2010 *Chins. Phys.* B **19** 104001

[11] Bliek D J, Botten L C, Deleuil R, MePhedran R C and Mayetre D 1980 *IEEE. Trans. Microwave Theory Technol.* **MTT-28** 1119

[12] Angelsky O, Mokhun A, Mokhun I, Soskin M and Luneburg R K 1996 *Mathematical Theory of Optics* (Berkeley: University of California Press)